Proof of Concept Experiments of Joint Waveform Design for Integrated Sensing and Communications

Tongyang Xu
Newcastle University
Newcastle upon Tyne, UK
tongyang.xu@ieee.org

Fan Liu
Southern University of Science and Technology
Sehnzhen, China
liuf6@sustech.edu.cn

Christos Masouros
University College London
London, UK
c.masouros@ucl.ac.uk

Izzat Darwazeh
University College London
London, UK
i.darwazeh@ucl.ac.uk

ABSTRACT

We design and test over-the-air for the first time, a joint dual-functional radar communication waveform for an integrated radar sensing and multi-user multiple input multiple output (MIMO) based orthogonal frequency division multiplexing (OFDM) communication system. Unlike existing work, the prototyping testbed in this paper can realize radar sensing and communication using the same time, frequency and spatial resources. The designed dual-functional integrated sensing and communication (ISAC) waveform in this work can be easily incorporated into existing communication standards where OFDM is used. The experiment observes a graceful trade-off between radar sensing and communication after comprehensive measurement on communication constellation diagrams and radar beampattern quality. This experiment also reveals the mutual impacts between communication signals using different modulation schemes and radar beampattern performance.

CCS CONCEPTS

• **Hardware** → **Signal processing systems**; • **Human-centered computing** → **Ubiquitous and mobile devices**.

KEYWORDS

Waveform, communications, radar, sensing, integrated sensing and communications (ISAC), OFDM, MIMO, software-defined radio (SDR), over-the-air, prototyping

1 INTRODUCTION

Integrated multi-function systems can save hardware, spectral and timing resources leading to superior resource efficiency over traditional single-function targeted systems. Signal communication is the basic function in transmission systems and specific standards are required to regulate the communication protocols. Radar sensing is an important application in military and healthcare areas, with an increasing application space in smart city and smart mobility. Commonly, resource multiplexing is applied to avoid mutual interference between communications and radar sensing but at the expense of separate hardware facilities and potentially frequency overlapping interference. Therefore, an integrated sensing and communication (ISAC) framework is of great importance to next generation communication systems.

A number of research efforts, aiming to design and test signalling that is appropriate for ISAC, have been investigated. Work in [5] aims to make use of empty subcarriers from communication signal frames for radar sensing pilot signals. Work in [9] proposed to use primary synchronization signal (PSS) in the LTE frame for the radar sensing purpose. Work in [6] proposed a scheme that can support radar sensing and communications by sending spatially orthogonal beams. Work in [7] multiplexes low out-of-band power emission signals with radar signals in frequency domain to achieve ISAC. Work in [3] proposed to achieve joint communication and radar functions through index modulation.

This work aims to practically validate a new design framework for ISAC using a dual functional waveform design methodology. The initial theory has been comprehensively explored by [4] with the experiment validation in [8]. Unlike traditional phased array radar and communications, this work integrates digital precoding in MIMO communications, which improves spatial degrees of freedom and enables advanced signal processing. To have better understanding of ISAC in real-world scenarios, this work explores different modulation formats and the mutual effect between modulation constellation performance and radar beampattern quality.

2 DUAL FUNCTIONAL WAVEFORM DESIGN

2.1 Communication Model

The traditional MIMO communication model is the following

$$Y = H\tilde{X} + W, \tag{1}$$

where $\mathbf{Y} = [\mathbf{y}_1, \mathbf{y}_2, ..., \mathbf{y}_K]^T \in \mathbb{C}^{K \times L}$ indicates K user side sample vectors with L samples per user. $\mathbf{H} = [\mathbf{h}_1, \mathbf{h}_2, ..., \mathbf{h}_K]^T \in \mathbb{C}^{K \times N}$ is a MIMO channel matrix wgere N indicates the number of transmitter side antennas. $\tilde{\mathbf{X}} = [\tilde{\mathbf{x}}_1, \tilde{\mathbf{x}}_2, ..., \tilde{\mathbf{x}}_N]^T \in \mathbb{C}^{N \times L}$ is the intended transmission symbol matrix where L is the number of time samples per data stream on each antenna. $\mathbf{W} = [\mathbf{w}_1, \mathbf{w}_2, ..., \mathbf{w}_K]^T \in \mathbb{C}^{K \times L}$ is the noise matrix including K receiver side user noise vectors. The expression in (1) can be further transformed into

$$\mathbf{Y} = \mathbf{X} + \underbrace{(\mathbf{H}\tilde{\mathbf{X}} - \mathbf{X})}_{MUI} + \mathbf{W}, \tag{2}$$

where $\mathbf{X} = [\mathbf{x}_1, \mathbf{x}_2, ..., \mathbf{x}_K]^T \in \mathbb{C}^{K \times L}$ indicates the user side symbol matrix. The second term on the right side hand in (2) represents the MUI term and the total power contributed by the MUI terms is computed as

$$P_{MUI} = \left\| \mathbf{H}\tilde{\mathbf{X}} - \mathbf{X} \right\|_F^2, \tag{3}$$

where $\|\cdot\|_F$ denotes the Frobenius matrix norm. The value of P_{MUI} indicates interference and in order to have better performance at the user side, the value of P_{MUI} should be minimized.

2.2 Radar Sensing Model

The design of a radar beam waveform is equivalent to the design of the spatial covariance matrix [2] of probing signals, and the spatial covariance matrix of $\tilde{\mathbf{X}}$ has the following expression

$$\mathbf{R}_d = \frac{1}{L}\tilde{\mathbf{X}}\tilde{\mathbf{X}}^H, \tag{4}$$

where a radar beampattern is determined by $\mathbf{R}_d$ and the its value should be positive-definite and should meet $L \geq N$.

To achieve the dual-functional sensing and communications, we need to optimize the transmission symbol matrix $\tilde{\mathbf{X}}$, which can minimize P_{MUI} in (3) and simultaneously approximate the radar beampattern based on the constraints in (4).

For an omnidirectional radar beampattern, the transmission waveform matrix $\tilde{\mathbf{X}}$ has to be orthogonal leading to an identity covariance matrix. Therefore, a dual-functional waveform on radar communication can be obtained via the following optimization

$$\begin{aligned} \min_{\tilde{\mathbf{X}}} \quad & \left\| \mathbf{H}\tilde{\mathbf{X}} - \mathbf{X} \right\|_F^2 \\ \text{s.t.} \quad & \frac{1}{L}\tilde{\mathbf{X}}\tilde{\mathbf{X}}^H = \frac{P_T}{N}\mathbf{I}_N \end{aligned} \tag{5}$$

where P_T indicates the total transmission power and $\mathbf{I}_N$ is an $N \times N$ identity matrix. The above minimizes the communication MUI, while maintaining the ideal radar waveform.

For a directional radar beampattern design, a unique covariance matrix $\mathbf{R}_d$ is considered in the joint optimization problem as

$$\begin{aligned} \min_{\tilde{\mathbf{X}}} \quad & \left\| \mathbf{H}\tilde{\mathbf{X}} - \mathbf{X} \right\|_F^2 \\ \text{s.t.} \quad & \frac{1}{L}\tilde{\mathbf{X}}\tilde{\mathbf{X}}^H = \mathbf{R}_d, \end{aligned} \tag{6}$$

where $\mathbf{R}_d$ is positive-definite and its design is detailed in [2].

It is noted that the optimization problems in (5) and (6) enforce an equality constraint on the signal covariance, which will give a perfect design of a desired radar beampattern but the communication performance would be compromised.

2.3 ISAC Model

To flexibly achieve joint optimization of the communication model and the radar beampattern model, we introduce a trade-off parameter termed $0 \leq \gamma \leq 1$, where its value indicates the trade-off factor that balances the communication and radar performance as the following

$$\begin{aligned} \min_{\tilde{\mathbf{X}}} \quad & \gamma \left\| \mathbf{H}\tilde{\mathbf{X}} - \mathbf{X} \right\|_F^2 + (1 - \gamma)\left\| \tilde{\mathbf{X}} - \mathbf{X}_d \right\|_F^2 \\ \text{s.t.} \quad & \frac{1}{L}\left\| \tilde{\mathbf{X}} \right\|_F^2 = P_T, \end{aligned} \tag{7}$$

where the first term, $\left\| \mathbf{H}\tilde{\mathbf{X}} - \mathbf{X} \right\|_F^2$ aims to minimize the MUI while the second term $\left\| \tilde{\mathbf{X}} - \mathbf{X}_d \right\|_F^2$ aims to enforce the signal waveform to approach the desired radar waveform $\mathbf{X}_d$.

3 EXPERIMENT DESIGN FOR DUAL FUNCTIONAL ISAC WAVEFORM

The indoor experiment setup of this work is demonstrated in Fig. 1 where the designed MIMO-OFDM platform is equipped with N=6 transmitter antennas and K=2 users working at 2.4 GHz carrier frequency. The transceiver in Fig. 1(a) has an array of six omnidirectional antennas, which are placed in a uniform linear array (ULA) format at the top with the spacing of half wavelength. To explore the spatial diversity, each antenna is connected to an independent RF chain within the USRP-RIO-2953R. The output from each USRP is fed to an omnidirectional antenna via a Vaunix LPS-402 programmable phase shifter. In this experiment, the phase shifter is merely used for holding the omnidirectional antenna without any phase control functions. In this experiment, the sampling rate of each signal from one RF chain is 20 MS/s. We test different modulation formats in QPSK, 8QAM and 16QAM to explore the potential impact from modulation schemes to the radar pattern performance. The number of data sub-carriers is 12 and the IFFT size is 128. In addition, each OFDM symbol packs 10 cyclic prefix (CP) samples at the beginning for channel effect mitigation.

Due to the indoor limited space, we focus the radar part of our experiment one measuring the quality of the radar beampattern rather than showing specific radar sensing applications. To assist the measurement, we place a directional 6 dBi log-periodic (LP) PCB antenna, working from 850 MHz to 6.5 GHz carrier frequency, in front of the USRP array platform. To measure the radar beampattern from the testbed, a microwave anechoic chamber will be the optimal solution. The multipath propagation effect will be greatly suppressed and the signal power measured at the radar measurement antenna mainly comes from the direct line-of-sight reception. In this case, the beampattern is more accurately plotted. However, this scenario will greatly affect the validation of the communication part since multipath is removed. Therefore, there is a trade-off for the measurement of communication and radar beampattern. This work focuses on the measurement in an indoor space since the main function of this experiment platform is for communications while the radar sensing is an add-on function integrated in the communication system. Although indoor signal multipath can be simply solved via digital signal processing, the indoor multipath might affects radar beampattern measurement since reflections would cause unexpected beampattern variations. To cut the signal
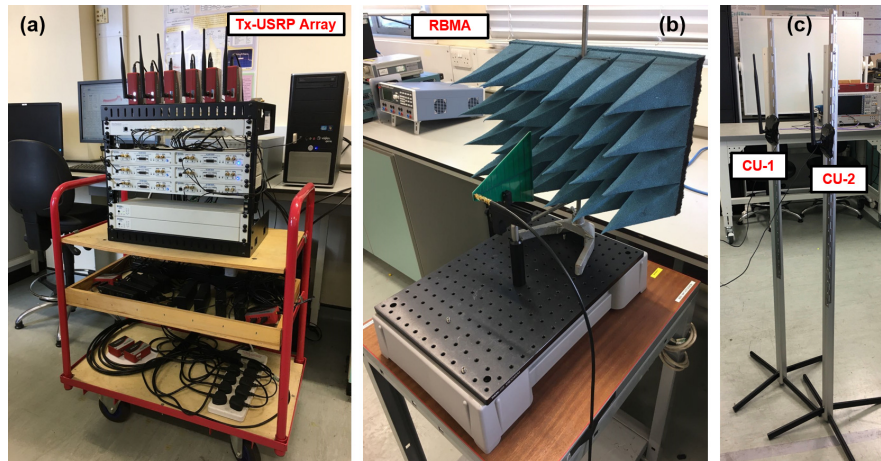
Figure 1: ISAC waveform experiment platform setup. (a) Tx-USRP Array: MIMO transceiver that precodes and decodes multi-user signals. (b) Radar Beampattern Measurement Apparatus (RBMA): a directional antenna to measure radar beampattern. (c) CU-1 and CU-2: two users that are quipped with omnidirectional antennas to receive communication signals.
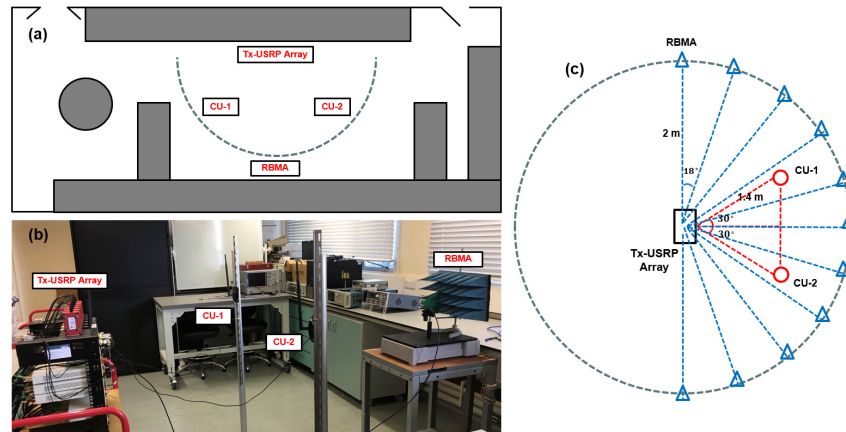
Figure 2: Radar beampattern measurement setup. (a) Laboratory floor plan. (b) Platform components arrangement. (c) Radar beampattern measurement diagram.

reflections to the radar beampattern measurement, we place a piece of radiation absorbing material (RAM) behind the LP antenna. The RAM can reduce signal reflections for signals working at central frequency between 1 GHz and 40 GHz. For the communication user side, we place two omnidirectional antennas in front of the testbed and each user is equipped with a single antenna.

The experiment measurement environment is demonstrated in Fig. 2 where the experiment space is approximately 4 m wide and 9 m long. There are many objects in the space that could cause signal reflections. The two users are placed nearly 1.5 m above the floor and are spaced at 1.4 m with each other and they are both 1.4 m away from the Tx-USRP array. The Tx side antenna array is around 1.5 m above the floor and the radar measurement antenna is placed 2 m away from the Tx-USRP array and is also 1.5 m above the floor. The radar beampattern measurement strategy is illustrated in Fig. 2(c) where the RBMA measures the signal power every 18

degrees with a radius of 2 m. Therefore, it will measure 10 points covering 180 degrees. It is noted that the platform employs small dipole antennas for signal transmission and the size of each dipole antenna is similar to one wavelength λ when considering the carrier frequency f_{RF}=2.4 GHz. Therefore, the beampattern measurement at a 2 m distance is greater than 2λ [1] and is practically within the far-field range. In addition, the 6 dBi LP PCB antenna with a narrow and focused radiation beam, can also mitigate the multipath effect for the radar beampattern measurement.

4 MEASUREMENT RESULTS

This work measures constellation patterns for QPSK, 8QAM, 16QAM and their constellation quality is used to evaluate the communication performance. In terms of radar beampattern, we will not only measure the radar beampattern at the Tx-USRP base station, but
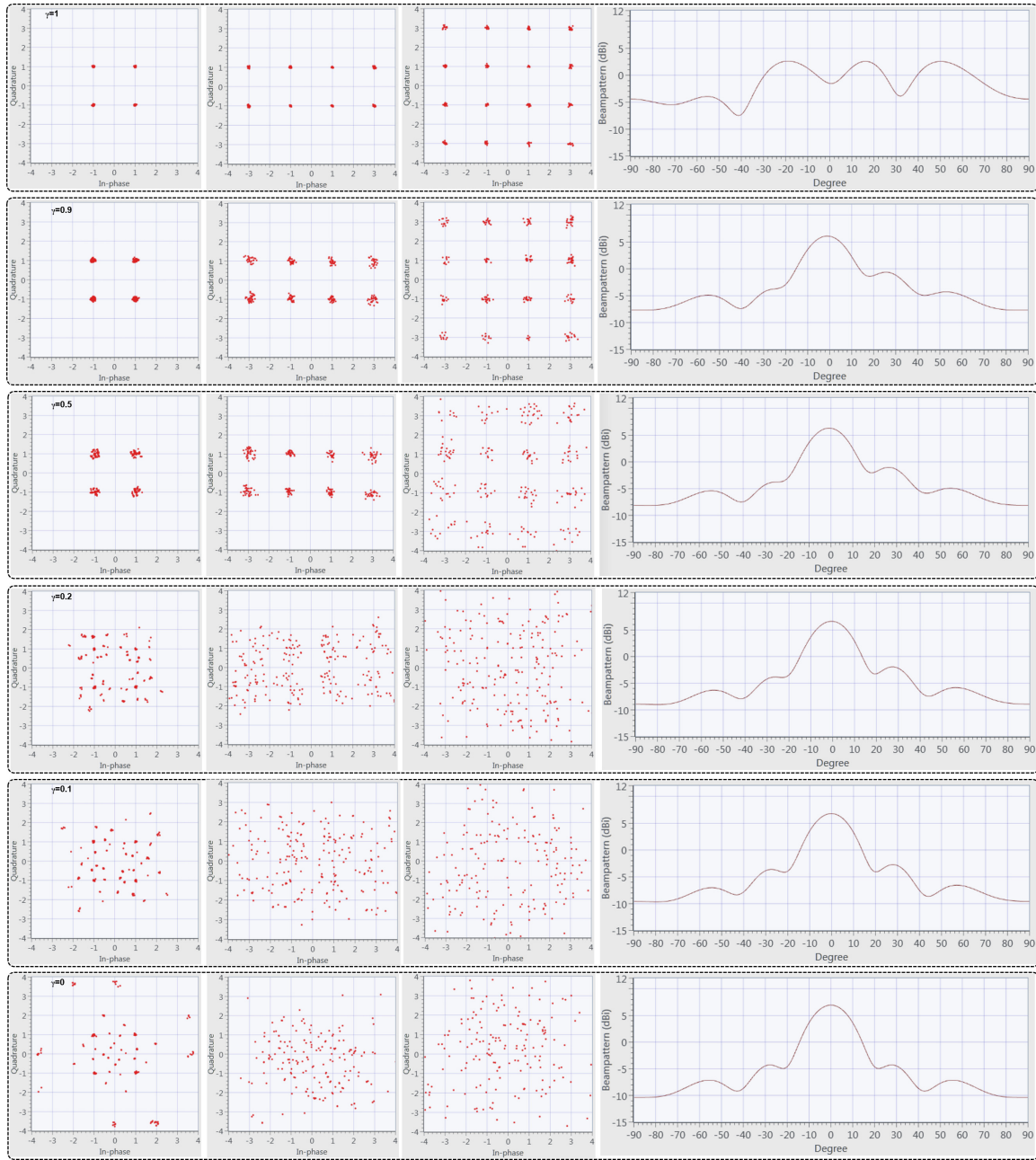
Figure 3: Measurement results at user side in terms of constellation diagram patterns (QPSK, 8QAM, 16QAM) and Tx-USRP side radar omnidirectional beampatterns at different values of trade-off factor γ.

also measure the beampattern at the RBMA, where signals would experience real-life distortions over the air.

Fig. 3 shows the user side recovered signal constellation patterns together with their corresponding transmitter side omnidirectional radar beampatterns at different values of the communication vs radar weighting factor γ. As observed in (7), high values of γ give priority to the communication functionality, while small γ values prioritise radar performance. It is observed that small values of

γ will degrade communication performance with more scattered constellation points. However, radar beampattern becomes better when the value of γ reduces. Fig. 4 shows the performance when directional radar beampatterns are equipped. When γ=0.2, 0.1, 0, the communication is greatly degraded because the constellation points are scattered and rotated. When γ is increased to 0.5, constellation points start to appear for low order modulation formats in QPSK and 8QAM. But for the densely packed 16QAM modulation

Figure 4: Measurement results at user side in terms of constellation diagram patterns (QPSK, 8QAM, 16QAM) and Tx-USRP side radar directional beampatterns at different values of trade-off factor γ.

scheme, the constellation points still scatter and indicate worse performance compared to other low order modulation formats. Further increasing γ to 0.9, constellation patterns become better for all the modulation schemes with a high quality of radar beampattern illustration. The relationship between EVM and the trade-off factor γ is presented in Fig. 5 where both directional and omnidirectional systems show reduced error vector magnitude (EVM) with the increase of γ.

Fig. 6(a) presents the graceful, scalable and controllable trade-off between the peak to sidelobe ratio (PSLR) of our designed directional radar beampattern and EVM. It is apparent that a high PSLR is obtained at the expense of worse EVM, which indicates a trade-off between radar beampattern quality and communication performance. It is observed in Fig. 6 (a) that γ=0.9 (PSLR=2.5 dB, EVM=-23.4 dB) balances the radar beampattern quality and communication performance. For omnidirectional performance in
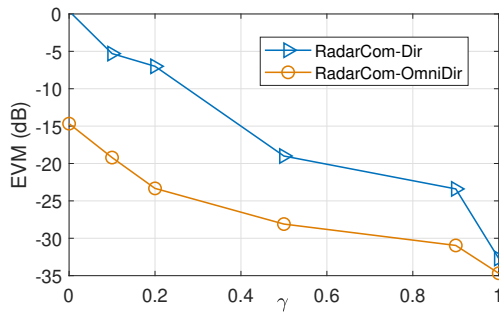
Figure 5: EVM measurement for omnidirectional and directional systems at various γ.
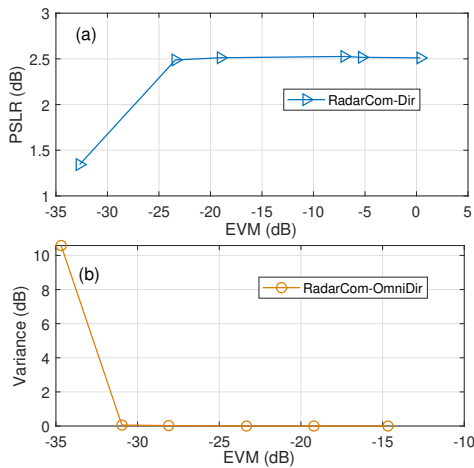

Figure 6: Investigations for the Trade-off design. (a) PSLR versus EVM in directional systems. (b) Variance versus EVM in omnidirectional systems.

Fig. 6(b), γ=0.9 (Variance=0 dB, EVM=-31 dB) shows the balance such that constellation points are clearly separated while the radar beampattern is in a perfect shape. In practice, the beampattern measurement at the RBMA is based on the received signal power. Since each signal includes real and imaginary samples, the power is calculated as $P = \frac{1}{Q}\sum_{k=1}^{Q}[\Re(x_k)^2 + \Im(x_k)^2]$, where x_k indicates the kth received complex symbol and $\frac{1}{Q}$ is the scaling factor for average power computation. $\Re(\cdot)$ and $\Im(\cdot)$ indicate the real part and imaginary part of a symbol, respectively.

The practical radar beampattern measurement at RBMA after the over-the-air transmission is demonstrated in Fig. 7 where the first subfigure shows clear directional baempattern and the second subfigure intends to show an omnidirectional beampattern but with power variations. It is expected to have better measurement quality when signal multipath is avoided.

5 CONCLUSION

An optimal trade-off factor is obtained to balance the performance for radar sensing and communications. Based on obtained results,
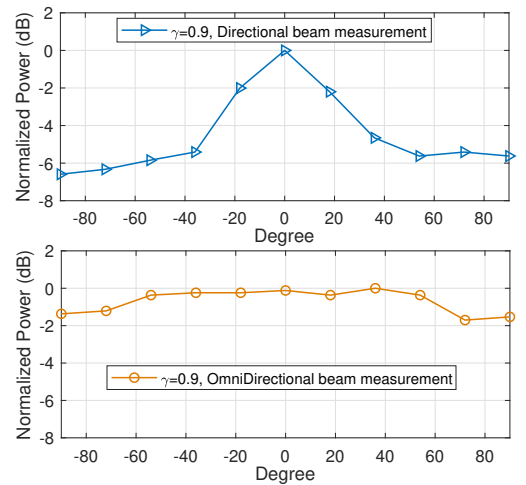

Figure 7: Measured omnidirectional and directional radar beampatterns when γ=0.9.

it is apparent that with the increase of the trade-off factor, communication performance is improved gradually with the improved quality of symbol constellation diagrams. This is due to the fact that a larger value of the factor will trade radar beampattern accuracy for better communication performance. When a small trade-off factor is used, the communication performance will be traded for better radar beampattern accuracy. The experiment also reveals that different modulation schemes have no effect to the quality of radar beampattern while the higher order modulation format would be easily affected by the trade-off fractor.

REFERENCES

[1] Constantine A. Balanis. 2016. . John Wiley & Sons. https://app.knovel.com/hotlink/toc/id:kpATADE01N/antenna-theory-analysis/antenna-theory-analysis
[2] Daniel R. Fuhrmann and Geoffrey San Antonio. 2008. Transmit beamforming for MIMO radar systems using signal cross-correlation. *IEEE Trans. Aerospace Electron. Systems* 44, 1 (2008), 171–186.
[3] Tianyao Huang, Nir Shlezinger, Xingyu Xu, Yimin Liu, and Yonina C. Eldar. 2020. MAJoRCom: A Dual-Function Radar Communication System Using Index Modulation. *IEEE Transactions on Signal Processing* 68 (2020), 3423–3438.
[4] Fan Liu, Longfei Zhou, Christos Masouros, Ang Li, Wu Luo, and Athina Petropulu. 2018. Toward Dual-functional Radar-Communication Systems: Optimal Waveform Design. *IEEE Transactions on Signal Processing* 66, 16 (2018), 4264–4279.
[5] Sahan Damith Liyanaarachchi, Taneli Riihonen, Carlos Baquero Barneto, and Mikko Valkama. 2021. Optimized Waveforms for 5G-6G Communication with Sensing: Theory, Simulations and Experiments. *IEEE Transactions on Wireless Communications* (2021), 1–1.
[6] Patrick M. McCormick, Shannon D. Blunt, and Justin G. Metcalf. 2017. Simultaneous radar and communications emissions from a common aperture, Part I: Theory. In *2017 IEEE Radar Conference (RadarConf)*. 1685–1690.
[7] Jessica B. Sanson, Daniel Castanheira, Atio Gameiro, and Paulo P. Monteiro. 2019. Non-Orthogonal Multicarrier Waveform for Radar With Communications Systems: 24 GHz GFDM RadCom. *IEEE Access* 7 (2019), 128694–128705.
[8] Tongyang Xu, Fan Liu, Christos Masouros, and Izzat Darwazeh. 2022. An Experimental Proof of Concept for Integrated Sensing and Communications Waveform Design. *ArXiv* abs/2202.04602 (2022).
[9] Qixun Zhang, Huan Sun, Zhiqing Wei, and Zhiyong Feng. 2020. Sensing and Communication Integrated System for Autonomous Driving Vehicles. In *IEEE INFOCOM 2020 - IEEE Conference on Computer Communications Workshops (INFOCOM WKSHPS)*. 1278–1279.